Proc. QCTM, Fukui 1993
J. Phys. Soc. Jpn. 63(1994) Suppl. A pp. 244 – 252

Nano-Structure Fabrication for Advanced III-V Semiconductor Devices

Tomonori ISHIKAWA
Optoelectronics Technology Research Laboratory
5-5 Tohkodai, Tsukuba, Ibaraki 300-26, Japan

The requirements of fabrication technology for nanometer structure devices with III-V compound semiconductors are described. In addition to fabrication capability with nanometer accuracy, the processes are required to avoid unintentional contaminations and any damage effect. To meet these requirements we have developed "*in-situ* EB lithography" in which all of the processes, including lithography, etching and epitaxial overgrowth, are performed successively in a UHV environment. The present status of this technique, i.e. $50nm$ patterning, cleanliness of the processed surfaces and damage-free characteristics, is shown.

1. Introduction

There has been much attention to semiconductor ultrafine structures, being motivated by future optoelectronic device applications[1,2]. Mesoscopic devices, based on submicron- or nanometer-sized structures, are attractive candidates for future functional devices with high performance. Recent progresses concerning microfabrication techniques combined with epitaxial growth techniques having atomic-scale controllavility have made possible the fabrication of such structures. However, we must also pay much attention to minimizing any undesirable effect of the surface-states, as well as crystal-defects induced during the fabrication processes since they seriously degrade the electrical and optical properties of ultrafine structures[3,4]. Especially, chemical changes due to contamination at the surface must be avoided, since III-V compound semiconductors are sensitive to them and the ratio of the surface to the entire volume becomes very high in our targeted nano-structures. Therefore, the entire fabrication process of a semiconductor ultrafine structure should most desirably be performed in a vacuum chamber without being exposed to air. This is the concept of the so-called "through ultra-high vacuum (UHV) processing" or "UHV *in-situ* processing"[5,6,7].

In this context, research on UHV *in-situ* processing using a focused-ion beam (FIB) was carried out. However, these ion-assisted processes inevitably introduce nonnegligible damage into the base materials. For example, FIB-assisted etching introduces a degradation of the photoluminescence (PL) intensity, by more than one-order of magnitude, even at $10keV$ ion energy, which

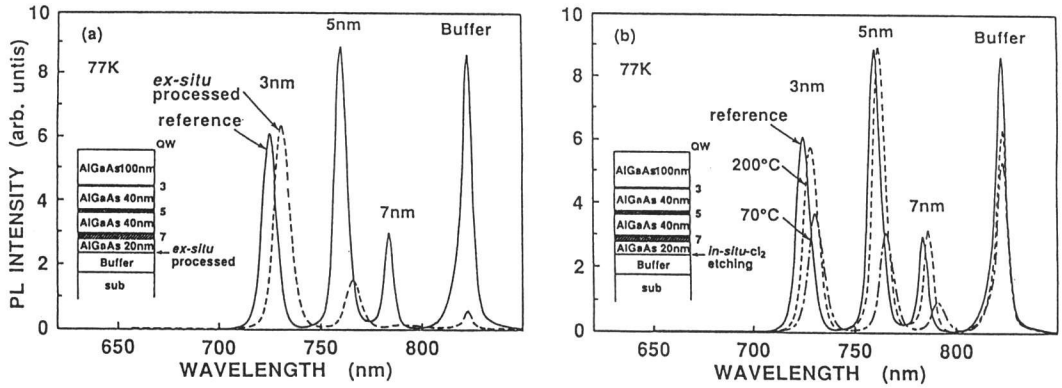

Fig.1.(a) PL spectra of an *ex-situ* processed MQW sample and a reference MQW sample. (b) PL spectra of *in-situ* Cl_2-etched MQW sample and a reference sample.

is the minimum energy required for focusing the FIB to less than $100nm$[8]. We have therefore developed a lithography process using a focused electron-beam (EB) instead of an FIB, as a UHV *in-situ* processing for a GaAs-AlGaAs system. In this lithography, which we call "*in situ* EB lithography"[6,9,10], an ultrathin surface-oxidized layer of GaAs is used as both the resist film and the etching mask, which can be patterned by EB-induced Cl_2 etching and can be removed by heating . The basic process of *in situ* EB lithography is a local removal of the surface oxide layer of GaAs by simultaneous irradiation of EB and Cl_2 gas.

In this paper we describe the UHV *in-situ* processing technology, while focusing on *in-situ* EB lithography. First, we demonstrate the advantage of UHV *in-situ* processes over the conventional processes regarding cleanliness of the processed surfaces. We then describe the damage-free characteristics of the EB-based processes. Finally, we describe the recent achievements of *in-situ* EB lithography. By using an EB with focusing characteristics of less than $40nm$, together with ultrathin GaAs oxide mask layers, fine-pattern formation of GaAs with a dimension as small as $50nm$ has been successfully demonstrated.

2. Assessment on the Cleanliness of the Processed Surfaces

To confirm the advantage of UHV *in-situ* processes, in this section we give an assessment of the cleanliness of *in-situ* processed surfaces. The lateral fine patterns which are commonly formed by dry-etching techniques, such as Cl_2-gas etching, must be buried by a successive overgrowth of wide-gap materials (so-called buried structures) to fabricate carrier confinement structures. In these processes the etched/regrown interfaces must be clean to avoid any electrical or optical degradations which are fatal for ultrafine structures. To meet this requirement, all of the processes should most desirablly be performed in a UHV or high-pure-gas enviroment without air-exposure. Here, we describe the cleanliness for various processed/regrown interfaces, while focusing on *in-situ* Cl_2-gas etched/regrown interfaces[11].

Figure 1(a) shows the photoluminescence (PL) spectrum of a multi-quantum-well (MQW) structure grown on a conventionally treated (*ex-situ* processed) GaAs buffer layer, together with that of a continuously grown sample as a reference. The series of light emission corresponds

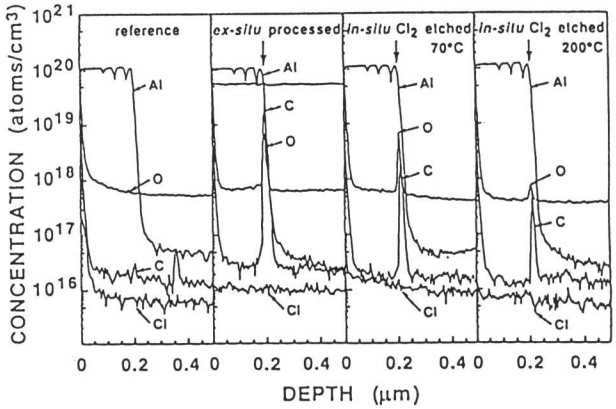

Fig.2. Impurity profiles of *in-situ* Cl_2-etched MQW samples, an *ex-situ* processed MQW sample and a reference MQW sample obtained by SIMS

to three QWs with well widths of 3, 5 and $7nm$ and GaAs buffer layer. In the preparation of an *ex-situ* processed sample, the molecular beam epitaxy (MBE)-grown buffer layer was air-exposed and wet-treated for cleaning, then followed by the MBE growth of an MQW structure. For this sample, drastic degradations of the PL intensity were observed, especially for the buffer layer and a $7nm$-QW, while no degradation was observed for the top $3nm$-QW, compared to a reference sample. For the *in-situ* Cl_2-etched sample(Fig.1(b)), on the other hand, especially for $200°C$ etching, the optical degradation was not so serious, indicating the advantage of *in-situ* Cl_2-gas etching over the conventional air-exposed processes.

These results concerning the optical properties can be explained in terms of an impurity accumulations induced during the processing. Figure 2 shows secondary-ion mass spectroscopy (SIMS) depth profiles of the MQW samples used in the PL measurement in Fig.1. In the etched samples and the *ex-situ* processed sample, carbon (C) and oxygen (O) were detected at the processed/regrown interfaces. We found a considerable amount of C and O accumulations at the interface for the *ex-situ* treated sample, with peak concentrations of $3 \times 10^{19} atoms/cm^3$ and $7 \times 10^{18} atoms/cm^3$, respectively. These impurities absorbed by air-exposure are considered not to be able to be completely removed by the thermal cleaning technique before MBE growth. For the *in-situ* Cl_2 etched sample, on the other hand, the impurity concentrations were reduced due to the avoidance of oxidation/contamination. Especially for a sample etched at $200°C$, a remarkable reduction of the impurities was achieved due to the high volatilities of the reaction products.

From the above-mentioned results, a UHV *in-situ* process technique, such as "*in-situ* EB lithography", which can avoid air-exposure, was proven to have an advantage in fabricating ultrafine structures with high quality over the conventional techniques.

3. Characterization of EB-Induced Damages

EB is expected to induce less-damage into GaAs/AlGaAs systems compared to FIB due to its small mass. However, they must be strictly assessed, since the nano-structures are very sensitive to any crystal defect as to the surface contaminations. Therefore, the effects of keV-

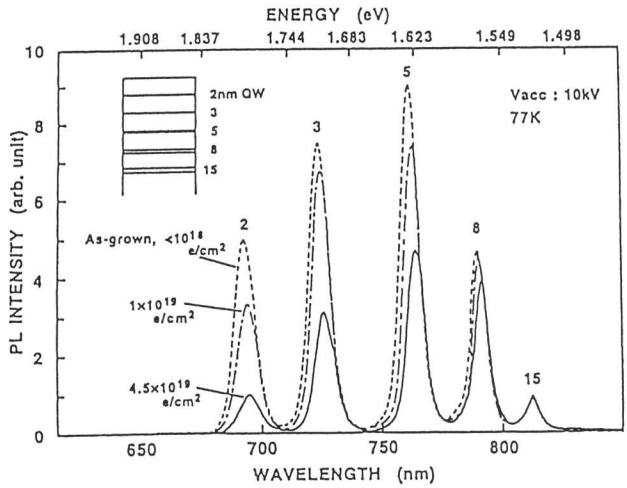

Fig.3. PL spectra of the as-grown and the $10keV$-EB irradiated GaAs/AlGaAs QW-structure samples.

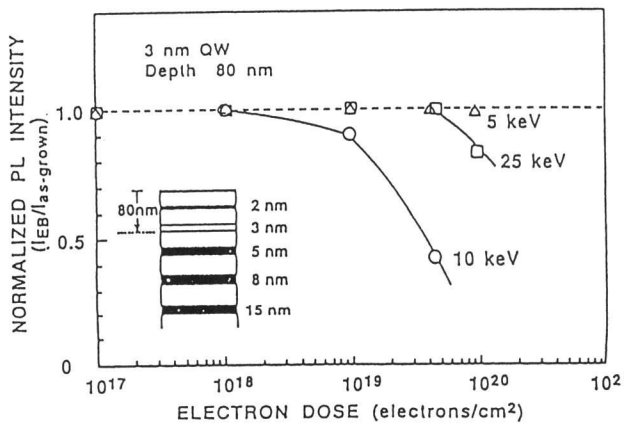

Fig.4. Normalized PL intensity of EB irradiated QW structures as a function of the electron dose.

range EB irradiation were investigated for a wide range of electron doses[12]. Figure 3 shows the effect of EB irradiation on the PL spectra ($77K$) of GaAs/AlGaAs quantum wells (QWs) having the structure shown in the figure. The series of light emission corresponds to five QWs with well widths of $2, 3, 5, 8$, and $15nm$, respectively, located at different positions from the surface. Upon $10keV$ EB irradiation at a dose below $1 \times 10^{18} electrons/cm^2$, the PL intensity does not decrease compared to that of an unirradiated sample. When the dose is increased to $1 \times 10^{19} electrons/cm^2$, the irradiation reduces the PL indensities of the shallower $2, 3, 5nm$-QWs, although the deeper 8 and $15nm$-QWs are slightly degraded. However, even at doses as high as $4.5 \times 10^{19} electrons/cm^2$ the PL intensities of the three thinner QWs are reduced by only a factor of 4 or 5. These results are far less severe compared to ion-beam-induced damage. EB-induced damage is thus shown to be negligible under any use of EB lithography, since the necessary doses for conventional EB lithography and the novel "*in-situ* EB lithography" are at most $1 \times 10^{16} electrons/cm^2$ and $1 \times 10^{17} \sim 1 \times 10^{18} electrons/cm^2$, respectively.

Figure 4 shows the EB dose dependence of the normalized PL intensity of $3nm$-QW at an $80nm$-

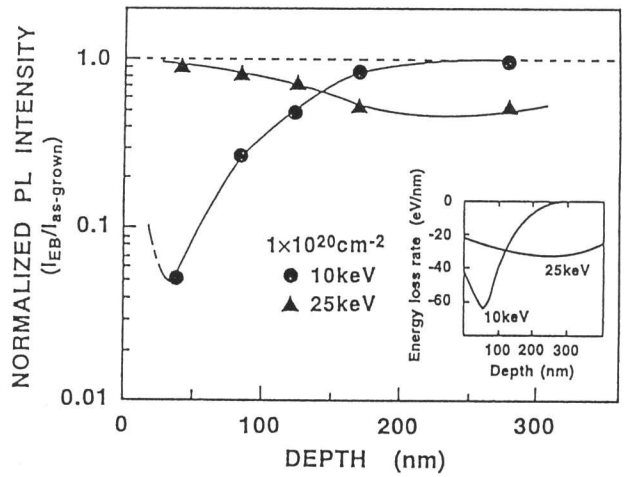

Fig.5. Depth dependence of PL intensity for QW structures irradiated by $10keV$- and $25keV$-electron beams.

depth beneath the surface irradiated at EB energies of $5, 10$ and $25keV$. The reduction of the PL intensity is most remarkable for $10keV$, at an electron dose of over $1 \times 10^{19} electrons/cm^2$. On the other hand, the PL intensity remains unchanged for $5keV$, and a slight PL intensity reduction is seen for $25keV$ upon increased doses of as high as $1 \times 10^{20} electrons/cm^2$. Such an energy dependence of the PL degradation can be explained in terms of the electron penetration depth and the energy-loss-distribution, depending on the EB energy. Namely, the $5keV$ electron penetration is too shallow to cause any damage in the QW regions. When the EB energy is increased up to $10keV$, electrons penetrate into the QW region and induce damage in it. As the energy increases, however, the energy-loss-rate decrease due to the reduced cross section of collisions with the target, resulting in a broadening of its distribution. Thus, at $25keV$, PL degradation does not become remarkable at $80nm$-depth from the surface; however, it becomes detectable at a deeper position of around $200nm$, where the energy-loss-rate for $25keV$ becomes maximum.

The depth dependence of the PL intensity for 10 and $25keV$ with a high dose of 1×10^{20} $electrons/cm^2$ is shown in Figure 5. The $10keV$-EB irradiation produces a more severe degradation in shallow QWs within $120nm$, since the energy-loss-rate sharply increases near the surface. At $25keV$, in contrast, the PL degradation is observed to be greater for deeper QWs. Thus, the higher energy EB-induced damage is shown to be deeply and broadly distributed with a maximum value at $200 \sim 300nm$-depth, reflecting the energy-loss-distribution of $25keV$. The calculated energy-loss-rate is also shown in the figure, and proven to be consistent with the PL results. A similar energy dependence of the EB irradiation effect was observed in the electrical properties, such as the 2DEG properties[13]. Thus, for keV-EB irradiation, the energy transferred from incident electrons to the target atoms creats defects which degrade both the optical and electrical properties.

4. In-situ EB Lithography

From the above-mentioned characterization of damagae, EB-assisted processes are proven to be damage-less. Also in section 2, UHV *in-situ* processes are shown to be advantageous for

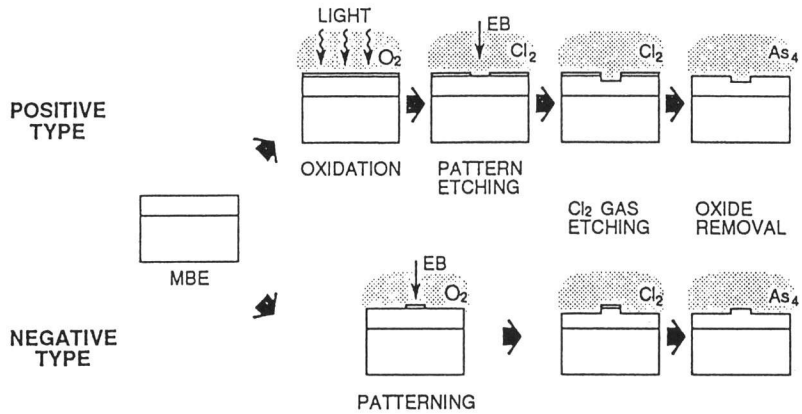

Fig.6. Illustration of the procedure for *in-situ* EB lithography. The upper and lower parts indicate positive- and negative-type lithography, respectively.

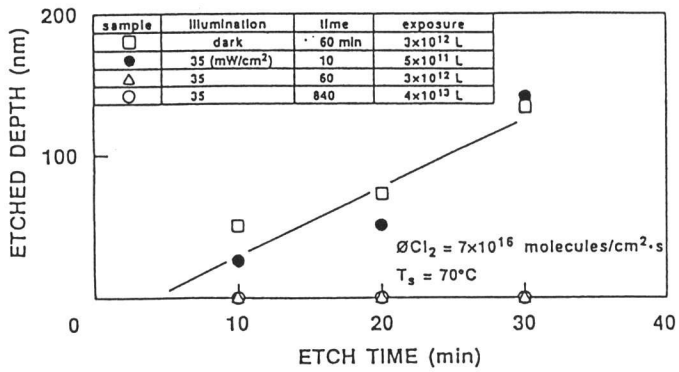

Fig.7. Etch depth of various photo-oxidized GaAs wafers as a function of the etch time.

obtaining a clean processed surface, which are indispensable for the fabrication of ultrafine structures with high optical quality. Thus, the EB-assisted process which are carried out in a UHV enviroment are promising for ultrafine structure fabrication. Here, "*in-situ* EB lithography"[6,9,10] is described as an example of such novel *in-situ* EB process.

There are two possible types of *in-situ* EB lithography: positive and negative. The upper part of Figure 6 illustrates the procedure of the positive type, including (1) preparation of a clean GaAs surface by MBE, (2) photo-oxidation of the surface, (3) direct patterning of the oxide by EB exposure with or without a Cl_2 ambient, (4) Cl_2 gas etching of the GaAs surface for pattern transfer, and (5) removal of any residual GaAs oxide layer by heating the wafer under arsenic pressure. The key point of this technique is that the GaAs oxide formed on the wafer surface by photo-oxidation fulfills the roles of both a resist film and an etching mask; it can be locally removed for patterning by EB irradiation and low-pressure Cl_2 gas exposure.

The durability of the oxide layer against Cl_2 gas exposure depends on the oxidation conditions, as shown in Figure 7. Four oxide layers prepared with various conditions exhibit different durabilities. For the samples prepared by oxidation in the dark and under illumination with a short time of 10 minutes, the etch depth increases with increasing the etch time, indicating unsatisfactory durability. On the other hand, no etching occurs in the samples with oxidation

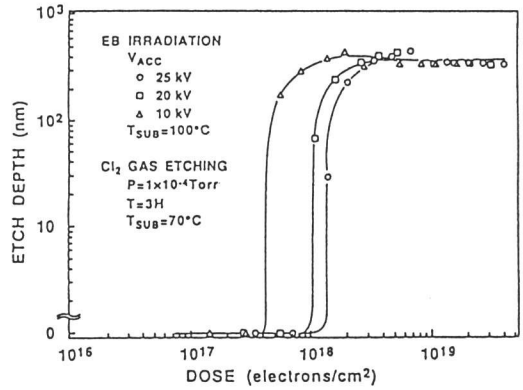

Fig.8. Variation of the etch depth as a function of the electron dose. The threshold dose for the initiation of etching increases as the electron energy increases.

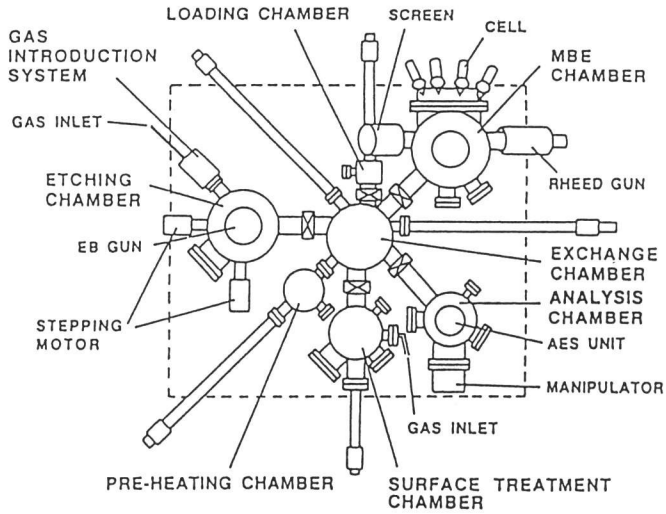

Fig.9. Schematic illustration of the UHV multichamber system used in *"in-situ* EB lithography".

under illumination for more than 60 minutes, indicating sufficient durability as an etching mask against Cl_2 gas. The cause of this difference in the durability may be attributed to the bonding of oxygen to GaAs as well as the thickness of the GaAs oxide layers.

The EB irradiation again weakens the durability of oxide layer against Cl_2 gas, making pattern formation possible. This is thought to be due to a partial desorption of oxygen from the oxide layer upon EB irradiation[14]. Figure 8 shows the etched depth in the two steps (3) and (4) plotted against the electron dose. A steep rise in the etching depth can be seen at around an electron dose of $3 \times 10^{17} cm^{-2}$, under which etching does not proceed. This threshold-like characteristic is quite favorable for fine-pattern lithography.

On the other hand, the procedure for negative-type lithography is shown in the lower part of Fig.6. Direct patterning is performed on a clean suface by EB irradiation under a low-pressure oxygen atmosphere. The resulting EB-stimulated oxide layer is resistive to the following Cl_2

gas etching, and also acts as an etching mask. The following processes are the same as that of the positive-type.

All of the above-mentioned processes are performed successively in a UHV-based multichamber system (Figure 9), comprising seven chambers used for etching, MBE growth, sample preheating, surface treatment, surface analysis, sample exchange, and sample loading. The base pressure of the system is better than $1 \times 10^{-9} Torr$, except for the loading chamber. The top of the etching chamber is equipped with an EB gun column.

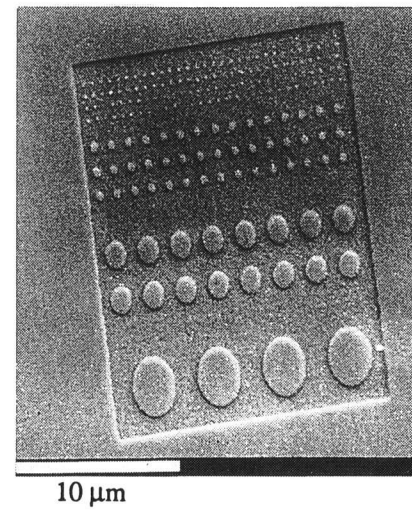

Fig.10. SEM photograph of a dot array formed on a GaAs surface. The minimum diameter of a dot is about $100nm$.

An example of a fine-pattern successfully fabricated by *in-situ* EB lithography is shown in Figure 10. It is an SEM micrograph of a dot array with several dimensions, fabricated by positive-type lithography. The minimum size of the dot diameter is as small as $100nm$. Moreover, a $50nm$ size pattern, which is almost equl to the EB spot size, has been obtained[15], indicating a smaller scattering effect of the incident electrons. This seems to be due to the very small thickness of the resist oxide-layer, which can avoid the electron-scattering effect in itself.

Together with such an excellent feasibility for fine pattern formation, the damage-free features and ultra-clean surfaces during processing make *in-situ* EB lithography promising for the fabrication of advanced devices based on nano-structures.

5. Summary and Future Prospects

UHV *in-situ* processes in which EB-induced patterning plays a central role have been developed as possible candidates to fabricate semiconductor nano-structures for future electronic and optoelectronic devices. The experimental results show that EB-assisted processes are the less-damage processes and that UHV *in-situ* processes are advantageous for obtaininig a clean processed surface, which is indispensable for the fabrication of nano-structures. Thus, EB-assisted processes in a UHV environment, such as *in-situ* EB lithography, are shown to be promising for future development. As the requirements for ultrafine structure become urgent, however, these techniques must be further developed so that the fabrication of a deep nanometer range can realized for mesoscopic device applications.

Acknowledgement

The author would like to thank N. Tanaka, H. Kawanishi, Y. Sugimoto for their great contributions in the present work.

References

1) H. Sakaki: Jpn. J. Appl. Phys. **19** (1980) L735.

2) Y. Arakawa and A. Yariv: IEEE J. Quantum Electron. **QE-22** (1986) 1887.

3) B. E. Maile, A. Forchel, R. Germann, D. Grutzmacher, H. P. Meier and J. -P. Reithmaier: J. Vac. Sci. Technol. **B7** (1989) 2030.

4) K. Ishibashi, H. Kawai, K. Gamo, S. Namba, S. Ishida, K. Murase, Y. Aoyagi and M. Kawabe: Sol. State. Commun. **63** (1987) 1169.

5) A. Takamori, E. Miyauchi, H. Arimoto, Y. Bamba, T. Morita and H. Hashimoto: Jpn. J. Appl. Phys. **24** (1985) L414.

6) K. Akita, Y. Sugimoto, M. Taneya, Y. Hiratani, Y. Ohki, H. Kawanishi and Y. Katayama: Proc. 1990 SPIE. **1392** 576.

7) L. R. Harriott, H. Temkin, Y. L. Wang, R. A. Hamm and J. S. Weiner: J. Vac. Sci. & Technol. **B8** (1990) 1380.

8) Y. Sugimoto, M. Taneya, K. Akita and H. Hidaka: J. Appl. Phys. **68** (1990) 6415.

9) M. Taneya, Y. Sugimoto, H. Hidaka, and K. Akita: J. Appl. Phys. **67** (1990) 4297.

10) H. Kawanishi, Y. Sugimoto, K. Akita, N. Tanaka and T. Ishikawa: Nanotechnology **3** (1992) 54.

11) N. Tanaka, I. Matsuyama, M. Lopez and T. Ishikawa: Proc. 1993 Int. Conf. on Solid State Devices and Materials, Chiba (1993) 760.

12) N. Tanaka, H. Kawanishi and T. Ishikawa: Jpn. J. Appl. Phys. **32** (1993) 540.

13) T. Fink, D. D. Smith and W. D. Braddok: IEEE Trans. Electrn Devices. **37** (1990) 1422.

14) H. Kawanishi, Y. Sugimoto, N. Tanaka and T. Ishikawa: Jpn. J. Appl. Phys. **31** (1992) 4444.

15) H. Kawanishi, Y. Sugimoto, N. Tanaka and T. Ishikawa: Jpn. J. Appl. Phys. **32** (1993) 4033.